

A comparative theoretical study on the solvent dependency of anthocyanin extraction profiles



Kim Phan^a, Elias Van Den Broeck^b, Katleen Raes^c, Karen De Clerck^d, Veronique Van Speybroeck^b, Steven De Meester^{a,*}

^aLaboratory for Circular Process Engineering (LCPE), Department of Green Chemistry and Technology, Ghent University Campus Kortrijk, Graaf Karel de Goedelaan 5, B-8500 Kortrijk, Belgium

^bCenter for Molecular Modeling, Ghent University, Technologiepark 46, B-9052 Zwijnaarde, Belgium

^cResearch Unit VEG-i-TEC, Department of Food Technology, Safety and Health, Ghent University, Campus Kortrijk, Graaf Karel de Goedelaan 5, B-8500 Kortrijk, Belgium

^dDepartment of Materials, Textiles and Chemical Engineering (MaTCh), Ghent University, Technologiepark 70A, B-9052 Zwijnaarde, Belgium

ARTICLE INFO

Article history:

Received 14 October 2021

Revised 20 January 2022

Accepted 21 January 2022

Available online 29 January 2022

Keywords:

Anthocyanins

COSMO-RS

Density Functional Theory (DFT)

Extraction

Solvent

ABSTRACT

Anthocyanidins and anthocyanins are flavonoids with nutritional, antioxidative and color properties that are present in various food products and biomass, such as food waste. The large chemical diversity amongst these molecules potentially leads to different affinities or activities in food and non-food applications. In order to characterize the extraction profile, advanced analytical techniques along with optimized separation procedures are required. Alternatively, theoretical tools can be applied for predicting the solubility or binding affinity of molecules in various reaction media. In this paper, the solubility of anthocyanidins and anthocyanins was analyzed by various theoretical tools such as group contribution methods (e.g., Hansen solubility parameters and Flory-Huggins interaction parameter (χ_{12})) and molecular modeling (e.g., static calculations based on Density Functional Theory (DFT) and COSMO-RS). It was found that COSMO-RS was able to give quantitative information on the solubility behavior within various pure solvents and it is able to describe the main intermolecular interactions between colorant and solvent, while Hansen solubility parameters were most appropriate to find the most optimal organic solvent–water mixture ratio. In general, solvents with electron-rich aromatic rings and/or containing electron donors, acting as hydrogen bond acceptors, showed the highest solubilizing power for anthocyanidins and anthocyanins.

© 2022 Elsevier B.V. All rights reserved.

1. Introduction

Anthocyanins belong to the most colorful group amongst flavonoids and are responsible for red till bluish colors in most flowers, higher plants, fruit and vegetables. The large chemical diversity amongst these dyes leads to compound specific properties such as color, stability toward external conditions (pH and temperature) and antioxidant activity. The variety of substitution patterns on the B-ring lead to six frequently occurring anthocyanidins (ACDs), i.e. cyanidin (Cy), delphinidin (Dp), malvidin (Mv), pelargonidin (Pg), peonidin (Pn) and petunidin (Pt) (Fig. 1). ACDs can also be found in their glycoside form (bonded to a sugar moiety) and are called anthocyanins (ACNs) [1]. The most stable form of ACNs, the flavylium cation, appears between pH 1 till 3 and displays the red color. Increasing the pH leads to isomerization via kinetic or thermody-

amic pathways. The former induces a subsequent deprotonation of the flavylium cation yielding purple-bluish neutral, monoanionic and dianionic quinoidal bases, while the latter results into light-yellow chalcone isomers as a consequence of the nucleophilic attack of a water molecule at the C₂-position of the flavylium cation [2,3,4,5].

Currently, several food products containing anthocyanins are frequently processed leading to a vast amount of by-products generated by fruit and vegetable processing industries, such as pomace during production of fruit juices or wine. Typically, anthocyanins are present within the outer layers (skin/peel) of fruit and vegetables. Those parts usually form the base of the pomace and are ideal sources for extraction to obtain these high added-value bioactive compounds. Next to their bioactivity, these molecules can also be applied as food colorants or in non-food applications such as pharmaceuticals, cosmetics, textiles and dye sensitized solar cells (DSSC) [6]. ACDs and ACNs are known to be beneficial for human health due to their antioxidant activities, but also have various

* Corresponding author.

E-mail address: Steven.DeMeester@UGent.be (S. De Meester).

Table 2

A summary of studies in which the solvent dependency on the ACN composition is investigated on the individual concentration level (EtOH: ethanol and MeOH: methanol).

Material	Solvent	ACNs					
		Cy3Glc	Dp3Glc	Mv3Glc	Pg3Glc	Pn3Glc	Pt3Glc
Grape skin extract ^a [18]	Water + 0.1% HCl	1.34	6.86	14.68	–	3.31	8.26
	60% EtOH + 0.1% HCl	1.64	7.65	18.05	–	4.11	9.38
	60% MeOH + 0.1% HCl	1.58	8.22	20.56	–	4.94	9.52
	MeOH/Acetone/Water/HCl: 40:40:20:0.1	1.74	7.73	15.81	–	3.35	7.17
	70% MeOH + 7% acetic acid	1.52	7.96	19.2	–	3.78	9.08
	70% MeOH + 0.1% TFA	1.58	8.34	19.74	–	3.91	9.46
Bilberry ^a [10]	MeOH/Water/Acetic acid 20:75:5	4.39	3.70	3.32	–	2.48	2.95
	MeOH/Water/Acetic acid 80:15:5	4.51	4.53	4.03	–	2.75	3.50
Lowbush blueberry ^a [10]	MeOH/Water/Acetic acid 20:75:5	0.27	0.25	0.79	–	0.23	0.36
	MeOH/Water/Acetic acid 80:15:5	0.34	0.57	0.86	–	0.25	0.57
Cranberry ^a [10]	MeOH/Water/Acetic acid 20:75:5	0.029	–	–	–	0.074	–
	MeOH/Water/Acetic acid 80:15:5	0.019	–	–	–	0.045	–
Blueberry ^b [19]		Cy3Gal	Mv3Ara	Mv3Glc	Mv3Gal	Pn3Glc	Pn3Ara
	60% Acetone	0.12	–	0.092	0.21	0.043	0.021
	70% Acetone	0.14	–	0.11	0.26	0.059	0.035
	80% Acetone	0.13	–	0.10	0.24	–	0.027
	60% EtOH	0.067	–	0.062	0.16	0.026	0.018
	70% EtOH	0.062	–	0.067	0.16	0.028	0.014
	80% EtOH	0.064	–	–	0.019	0.012	0.098
	60% MeOH	–	–	0.012	0.020	0.012	0.28
	70% MeOH	0.082	0.057	–	0.015	0.32	0.11
	80% MeOH	0.063	–	0.056	0.0043	0.26	0.019

^a : mg/g DW,^b : mg/g FW, TFA: trifluoroacetic acid, Ara: arabinoside, Gal: galactoside and Glc: glucoside.

Very little systematic information is available on the effect of solvent type on the subtype of ACDs and ACNs that are extracted. Knowing this is important, for example toward assessing the bioactivity of extracts. ACDs have a higher Oxygen Radical Absorbance Capacity (ORAC) value compared to ACN, which is ascribed to the unstable aglycone resulting in a higher reactivity. Very specific ACDs or ACNs play a selective role in combating enemy cells or curing infections [20]. Therefore, a compound-specific extraction could be performed to maximize the yield of one particular compound, compared to total anthocyanin content. However, the characterization and quantification of each individual anthocyanin would require a matrix clean-up, complete separation and identification by means of high advanced analytical methods such as HPLC–DAD–MS/MS. Besides that, a calibration curve is required for each compound requiring expensive analytical standards, which are not always commercially available [21].

Theoretical tools, are frequently applied for predicting the solubility or binding affinity of drugs and additives and developing formulations. Common tools are phase-solubility studies, quantitative-structure property relationships [22], Hansen solubility parameter calculations via group contribution method [23,24], Flory-Huggins interaction parameter (χ_{12}) [24], conductor-like screening model for real solvents (COSMO-RS), COSMO segment activity coefficient model (COSMO-SAC) [25], etc. In molecular modeling, solvation energies could be obtained via static calculations using an implicit solvation model or a more computationally expensive explicit solvation model by means of molecular dynamics in combination with the Free Energy Perturbation (FEP) method. The latter provides a better accuracy with errors in the range of -1 to 5.4 kJ mol⁻¹ compared to experimental data [26,27]. The error with implicit solvation (PCM) for polar organic molecules goes beyond 13 kJ mol⁻¹ as the following phenomena are still challenging to be determined: hydrogen bonds, solvent entropy and non-electrostatic solvent effects for aprotic solvents [27]. These models could be applied on the extraction process of ACDs and ACNs to predict which solvent would be most effective toward which molecule. Yet, these models have different grades of complexity, and there is no literature available that assesses which model would be preferred for this purpose.

In this context, this paper aims at using and comparing theoretical tools toward predicting the outcome of a solvent on the extraction process. For this purpose, the solubilities of 8 ACDs (i.e., cyanidin (Cy), delphinidin (Dp), malvidin (Mv), pelargonidin (Pg), peonidin (Pn) and petunidin (Pt)) and 2 deoxyanthocyanidins: apigenin (Ap) and luteolinidin (Lt)) and the 3-glycoside ACN form of the 6 main ACDs were screened toward their solubility in 30 solvents (Table S1) with the most common predictive models toward solubility [22], being the Hansen solubility parameters, Flory-Huggins interaction parameter (χ_{12}), static calculations based on Density Functional Theory and the COSMO–RS hybrid solvent model (Fig. 2). The results obtained from the various theoretical tools were matched against experimental ACDs- and ACNs-containing extract profiles in water and binary aqueous mixtures from literature. Additionally, the solubilities of glucose and pectin, representing monosaccharides and cell wall polysaccharides, were investigated. The best theoretical tool can be used as a benchmark for compound-specific extractions to direct the applications' demands.

2. Materials and methods

2.1. Group contribution methods

2.1.1. Hansen solubility parameters (HSP)

The solubility of a compound in a solvent can be predicted via various solubility theories such as Hildebrand and Scott, Burrell and Hansen. Hildebrand introduced the solubility parameter (δ) as the square root of the cohesive energy density (CED). The CED equals to the energy required to vaporize a mole of liquid per unit volume. The main shortcoming of this solubility parameter is the lack of describing polar and hydrogen bonding interactions. This is largely solved by accounting for the individual contributions for the calculation of the total energy of vaporization [24]. One of the most widely used approach to calculate the solubility of drugs, solvents, polymers, oils and surfactants is the Hansen solubility parameters (HSP) [28]. The affinity between a solute and solvent is described by three types of interactions and thus, three partial

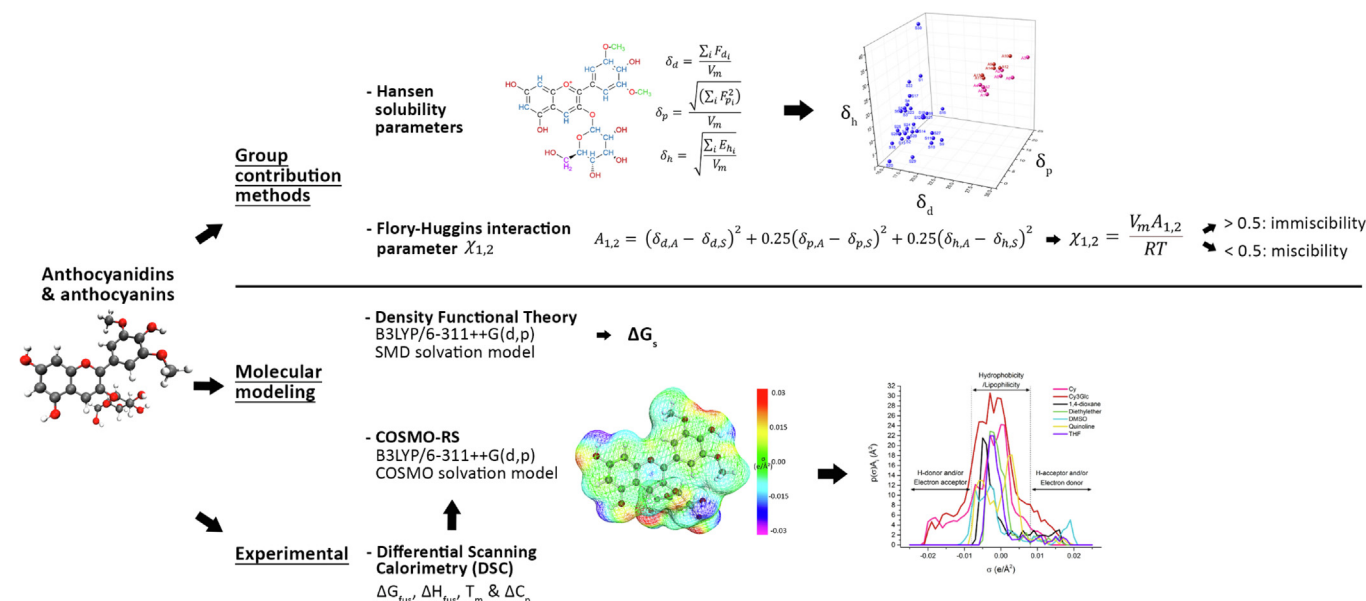


Fig. 2. Summary of the four applied theoretical tools required for predicting the solubility behaviour of anthocyanidins (ACDs) and anthocyanins (ACNs).

solubility parameters: dispersion (δ_d), polar (δ_p) and hydrogen bonding (δ_h). The individual HSPs were calculated based on the group contribution method of Hoftyzer and Van-Krevelen [23]:

$$\delta_d = \frac{\sum_i F_{d_i}}{V_m} \quad (1)$$

$$\delta_p = \frac{\sqrt{\sum_i F_{p_i}^2}}{V_m} \quad (2)$$

$$\delta_h = \frac{\sum_i E_{h_i}}{V_m} \quad (3)$$

where i represents the structural moiety within the molecule, F_{d_i} and F_{p_i} are the total group contributions for dispersion ($\text{J}^{1/2} \text{cm}^{3/2} \text{mol}^{-1}$) and polar ($\text{J}^{1/2} \text{cm}^{3/2} \text{mol}^{-1}$), respectively, E_{h_i} represents the group contribution to the hydrogen bonding energy (J mole^{-1}) and V_m is the molar volume of the molecule ($\text{cm}^3 \text{mole}^{-1}$).

The solubility parameter distance R_a in the Hansen space gives a qualitative view for the miscibility between solute and solvent (Fig. 3). The smaller R_a , the higher the miscibility between the two compounds of interest [24].

$$(R_a)^2 = 4(\delta_{d,A} - \delta_{d,S})^2 + (\delta_{p,A} - \delta_{p,S})^2 + (\delta_{h,A} - \delta_{h,S})^2 \quad (4)$$

where $\delta_{i,A}$ and $\delta_{i,S}$ ($\text{MPa}^{1/2}$) are the i^{th} component of ACDs/ACNs and solvent, respectively.

2.1.2. Flory-Huggins interaction parameter (χ_{12})

The Flory-Huggins “chi” parameter (χ) has been used for many years to define polymer blends. The χ_{12} interaction parameter, derived from the New Flory theory, is the successor of the χ -parameter and currently the standard for describing solute-solution behavior. This dimensionless parameter allows estimations where HSPs are known, but χ_{12} not. Hereby, the nonpolar Hildebrand solubility parameter for calculating χ_{12} is slightly modified by including HSPs containing polar and hydrogen bonding interactions, given by A_{12} (MPa) [24]:

$$A_{1,2} = (\delta_{d,A} - \delta_{d,S})^2 + 0.25(\delta_{p,A} - \delta_{p,S})^2 + 0.25(\delta_{h,A} - \delta_{h,S})^2 \quad (5)$$

with δ_d , δ_p and δ_h are dispersive, polar and hydrogen bonding solubility parameters calculated according to equations 1–3, respectively. This yields the following expression for calculating χ_{12} :

$$\chi_{1,2} = \frac{V_m A_{1,2}}{RT} \quad (6)$$

with V_m the molar volume of solvent (m^3/mol), R the gas constant ($\text{J}/\text{mol}\cdot\text{K}$) and T the temperature (K). The lower the χ_{12} -value, the better the miscibility between two compounds. More specifically, χ_{12} -values ≤ 0.5 indicate miscibility, while χ_{12} -values > 0.5 show immiscibility.

2.2. Molecular modeling

2.2.1. Density Functional Theory: Static calculations

Continuum solvation models such as PCM, COSMO or SMD are cost-effective methods for describing the electrostatic interaction between solute and solvent. Hereby, solvents are represented as a dielectric medium [26]. The dielectric constant (ϵ) has the biggest influence next to other solvent descriptors in the SMD implicit solvation model. All calculations were performed with Gaussian 16 [29] using density functional theory (DFT). Conformational analyses and frequency calculations were performed to find the absolute minimum for each ACD and ACN [30]. This was performed with the B3LYP [31,32] functional along with the 6-311++G(d,p) basis set, which has already proven its reliability in describing organic systems [33]. SMD is applied as implicit solvation model as this yields the most accurate solvation energies, but still comes with a mean unsigned error of 18.6 kJ mol^{-1} in solvation free energies for ions with B3LYP/6-31G* [34]. The solvation energies were calculated in the following ways:

$$\Delta G_{s,small} = G_{solvent} - G_{gas} \quad (7)$$

with G the free energy of the solute within the respective solvent and gas phase. This equation would only be suitable for small rigid molecules for which thermal contributions, derived from nuclear motion of the system, to the solute Gibbs free Energy are very similar in both gas and solution phase [35]. In systems where solvent-induced changes in thermal motions and the conversion of gas phase rotation to liquid phase librations are significant to the molecular structure, thermal corrections (G^{therm}) are explicitly

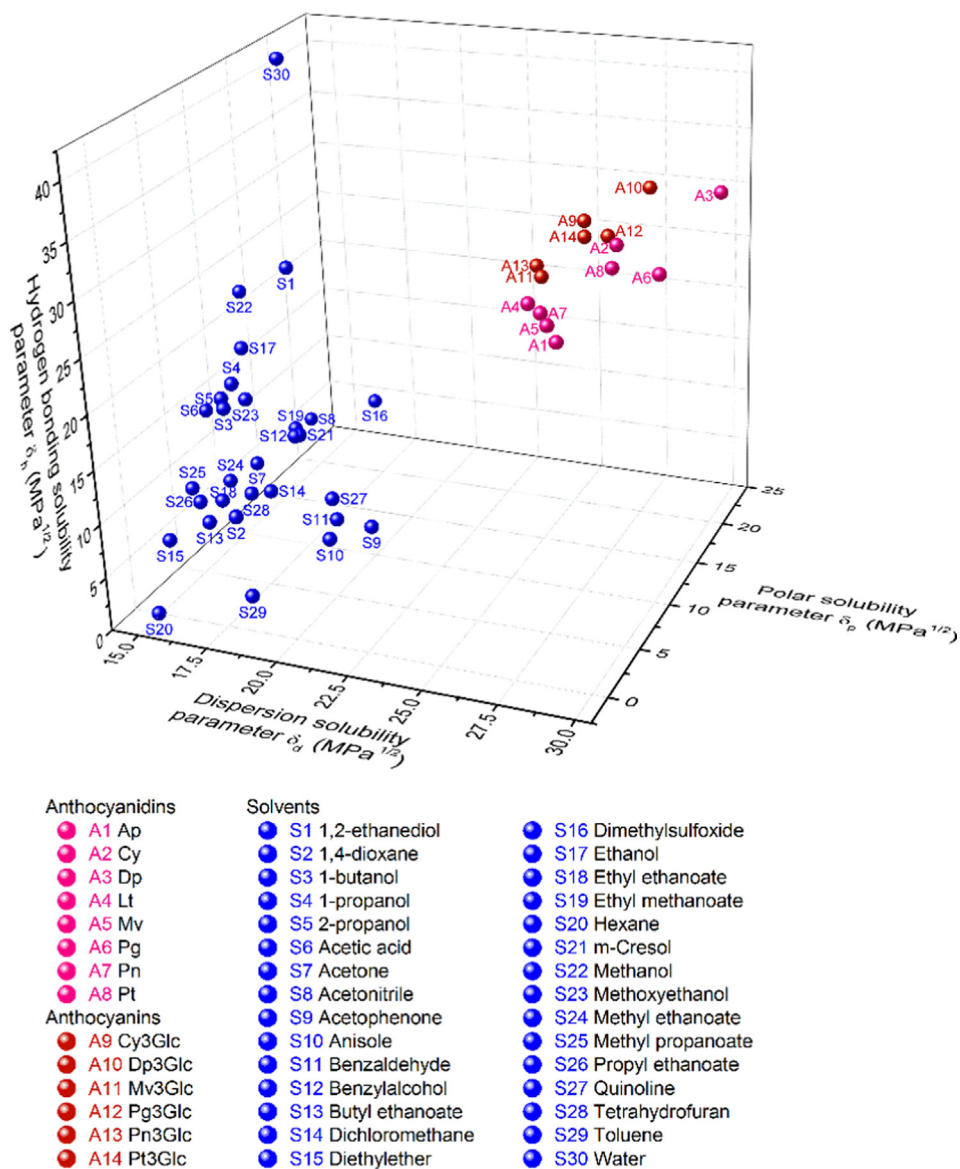


Fig. 3. Hansen solubility parameters (δ_d , δ_p and δ_h) of the selected solvents (blue dots labelled as S1-S30), ACDs (magenta dots labelled as A1-A8) and ACNs (red dots labelled as A9-A14). The smaller the distance R_a ($\text{MPa}^{1/2}$), the more likely the solvent will solubilize the ACDs or ACNs. Additional data are illustrated and tabulated in the supporting information (Fig. S3, Tables S3-S6).

taken into account and the calculated Gibbs free energy of solvation is more accurate [36]. Next to that, G_{nes} represents the non-electrostatic contributions such as cavitation and dispersion-repulsion interactions [35].

$$\Delta G_{s,large} = E_{solution} - E_{gas} + G_{solution}^{therm} - G_{gas}^{therm} + G_{nes} \quad (8)$$

where $E_{solution}$ and E_{gas} represent the solute electronic energies of the optimized geometries in solution and gas, respectively. Until now, researchers are able to parametrize hydration energies for neutral molecules, which match the experimental values, though elaboration to ionic compounds is more challenging [37].

2.2.2. Conductor-like screening model for realistic solvent (COSMO-RS)

This hybrid solvation model is based on conductor-like screening model (COSMO) calculations, introduced by Klamt (1995) [38] and is mostly applied for solubility prediction of drugs or formulations [39]. A COSMO-RS calculation starts with the COSMO implicit solvation model in which the molecule is surrounded by an infinite dielectric medium (perfect conductor). Afterward, the molecular

surface of the molecule is divided arbitrarily into segments for which the charge density of each surface element (σ_m) are calculated in this perfect conductor. Once the averaged value of σ_m has been obtained for each segment m , the probability $p(\sigma)$ is obtained by finding a given segment with a specified charge density multiplied with the entire surface area of the molecule ($p(\sigma)A_i$). The molecular interactions between solute and liquid are obtained by the statistical averaging of local pair wise interactions of surface segments. The COSMO files for ACDs, ACNs, glucose and pectin were generated by Gaussian 16 and processed with Biovia Cosmotherm 20.0.0 (Dassault Systèmes).

The accuracy for COSMO-RS calculations in determining the solubility for solid compounds can be increased by including experimental input about the phase change of the compounds from solid to liquid. The most important thermodynamic parameters are the free energy of fusion ΔG_{fus} , the enthalpy of fusion (ΔH_{fus}) and the melting temperature (T_m) and the change in heat capacity (ΔC_p). These thermodynamic parameters can be obtained via Differential Scanning Calorimetry (DSC) (*vide infra*). The free energy change at constant temperature is described:

$$\Delta G = \Delta H - T\Delta S. \quad (9)$$

Since at melting temperature, melting and crystallization processes are in equilibrium ΔG equals zero. As such

$$T_m = \frac{\Delta H_{fus}}{\Delta S_{fus}}. \quad (10)$$

which yields:

$$\Delta G_{fus} = \Delta H_{fus} - T \frac{\Delta H_{fus}}{T_m}. \quad (11)$$

The mole fraction solubility is calculated based on the free energy difference:

$$\ln(x_s) = \frac{(\mu_{pure} - \mu_s - \Delta G_{fus})}{RT}. \quad (12)$$

With μ_{pure} and μ_s representing the chemical potentials of the pure compound and the compound in solution, respectively; R the gas constant and T the temperature. The aforementioned chemical potentials can be derived by COSMO-RS. The reported COSMO-RS values are relative molar solubility values ($\log S_{RS}$ with $[S_{RS}] = \text{mol L}^{-1}$) obtained after conversion of the mole fraction solubility values ($\ln x_s$) via the molar volume of the solution. Overall, COSMO-RS is able to obtain solvation free energies in pure and solvent mixtures and avoid the more lengthy explicit solvent treatments. However, this model makes use of approximate parameters for nonelectrostatic contributions from cavitation, dispersion and repulsion, that were designed for neutral compounds, but recent developments show promising results for ionic liquids and electrolytes [40].

2.3. Experimental section

2.3.1. Reagents

Analytical standards of apigeninidin chloride ($\geq 97\%$), cyanidin chloride ($\geq 96\%$), delphinidin chloride ($\geq 97\%$), luteolinidin chloride ($\geq 95\%$), malvidin chloride ($\geq 97\%$), pelargonidin chloride ($\geq 97\%$), peonidin chloride ($\geq 97\%$), petunidin chloride ($\geq 95\%$), cyanidin-3-O-glucoside chloride ($\geq 96\%$), delphinidin-3-O-glucoside chloride ($\geq 95\%$), malvidin-3-O-glucoside chloride ($\geq 95\%$), pelargonidin-3-O-glucoside chloride ($\geq 95\%$), peonidin-3-O-glucoside chloride ($\geq 95\%$) and petunidin-3-O-glucoside chloride ($\geq 95\%$) were obtained from Extrasynthese (Genay, France).

2.3.2. Differential scanning calorimetry for COSMO-RS input

In order to obtain the melting properties of 14 ACDs and ACNs (ΔH_{fus} , T_m and ΔC_p), Differential scanning calorimetry (DSC) measurements were performed with the DSC 204 F1 system (NETZSCH). Samples of 2–4 mg were weighted in an aluminum crucible (25 μL) and subsequently sealed. The samples were heated from room temperature (25 $^{\circ}\text{C}$) up to 400 $^{\circ}\text{C}$ at a heating rate of 10 $^{\circ}\text{C min}^{-1}$ under constant flow of nitrogen, 20 mL min^{-1} . The thermograms were analyzed with NETZSCH Proteus Thermal Analysis (8.0.2) software to obtain the melting properties and are used as experimental input for COSMO-RS (Table S2 and Fig. S2).

2.3.3. Statistical analysis

The one-way analysis of variance (ANOVA) was carried out to investigate the added-value of the organic solvent of interest to the solubility compared to water. The significance level (α) for the statistical analyses is 0.05. The p-values obtained lower than 0.05 are regarded as significantly different. All statistical analyses were performed with SPSS Statistics Version 25 (IBM) software.

3. Results and discussion

3.1. Hansen solubility parameters and Flory-Huggins interaction parameter (χ_{12})

HSPs commonly display the smallest distances (R_a) for solvents that are most likely to solvate ACDs and ACNs (Figs. 3, S3 and Tables S3-S6). The following distances are average values per subclass of ACDs and ACNs ($R_{a,avg}$); 1,2-ethanediol ($R_{a,avg} = 20.88$), m-cresol (22.41), benzylalcohol (22.64) dimethylsulfoxide (DMSO) (22.92) and ethanol (24.23) are the preferred solvents for ACDs by applying the group contribution method. 1,2-ethanediol ($R_{a,avg} = 19.68$) is also the best solvent for ACNs followed by DMSO (22.84), m-cresol (23.23), benzylalcohol (23.46) and ethanol (23.85). It is clear that the most optimal solvents for ACN extraction put forward by the HSP method show a high structural resemblance with the natural dyes (i.e., aromatic rings and hydroxy groups). As this group contribution method is based on the structural fragments within a molecule, there are shortcomings for describing complex molecules wherein hydrogen bonds or electrostatic interactions occur [41]. The χ_{12} -values showed more polar solvents (i.e., alcohols) rather than aromatic solvents compared to HSPs. This model recommends water; 1,2-ethanediol; methanol, ethanol or DMSO as the five most optimal solvents for both ACDs ($\chi_{12} = 1.54, 2.54, 2.67, 3.59$ and 3.90 , respectively) and ACNs ($\chi_{12} = 1.22, 2.18, 2.36, 3.40$ and 3.80 , respectively), known their hydrophilic nature (Fig. S4 and Tables S7-S8). It can be noticed that all these χ_{12} -values are higher than 0.5. This trend corresponds to the χ_{12} -values obtained from Hong et al. (2015) [42]. These χ_{12} -values technically indicates immiscibility.

3.2. Density functional theory: Static calculations

The static calculations based on Gibbs free energies of solvation for small rigid molecules ($\Delta G_{s,small}$, equation (7)) recommend alcohols: methanol ($\Delta G_{avg,s,small} = -251.03 \text{ kJ mol}^{-1}$) > ethanol ($-249.42 \text{ kJ mol}^{-1}$) > 2-propanol ($-248.15 \text{ kJ mol}^{-1}$) > 1-propanol ($-246.20 \text{ kJ mol}^{-1}$) > 1-butanol ($-242.48 \text{ kJ mol}^{-1}$) for the eight ACDs (Fig. S5 and Tables S9-S13). Again, the given solvation energies are average values per subclass of ACDs and ACNs. The ranking for ACNs does not differ much compared to ACDs with methanol ($-310.95 \text{ kJ mol}^{-1}$) and ethanol ($-308.54 \text{ kJ mol}^{-1}$) being most efficient solvents, followed by water ($-305.07 \text{ kJ mol}^{-1}$), 2-propanol ($-302.36 \text{ kJ mol}^{-1}$) and 1-propanol ($-302.04 \text{ kJ mol}^{-1}$). The occurrence of water in the list confirms that additional hydroxy groups from the glucose moiety allows a better stabilization in water. The calculated Gibbs free energies of solvation also displayed smaller values for ACNs compared to ACDs with an extra 60 kJ mol^{-1} stabilizing energy in favor of ACNs for alcohols.

When thermal contributions and nonelectrostatic components are included for the Gibbs free energies of solvation ($\Delta G_{s,large}$, equation (8)), solvents with electron-rich aromatics appear as most optimal solvents in the case of ACDs: benzaldehyde $\Delta G_{avg,s,small} = -252.97 \text{ kJ mol}^{-1}$) > acetone ($-251.88 \text{ kJ mol}^{-1}$) > acetonitrile ($-251.67 \text{ kJ mol}^{-1}$) > quinoline ($-251.62 \text{ kJ mol}^{-1}$) > acetophenone ($-246.36 \text{ kJ mol}^{-1}$) (Fig. S6 and Tables S14-S17). For ACNs, the solubilizing power is as follows: acetone ($-298.19 \text{ kJ mol}^{-1}$) > 2-propanol ($-294.48 \text{ kJ mol}^{-1}$) > benzaldehyde ($-293.41 \text{ kJ mol}^{-1}$) > ethanol ($-291.93 \text{ kJ mol}^{-1}$) > acetonitrile ($-290.09 \text{ kJ mol}^{-1}$). Acetonitrile is an aprotic solvent, but contains π -electrons, which are also able to interact with the ACDs or ACNs π -systems. The solvation energies obtained from the calculations for the five most optimal solvents are all situated within a range of 10 kJ mol^{-1} .

3.3. Conductor-like screening model for realistic solvent (COSMO-RS)

The most optimal solvents according to COSMO-RS, expressed as the relative molar solubility values ($\log S_{RS}$ with $[S_{RS}] = \text{mol L}^{-1}$, for solubilizing ACDs are: tetrahydrofuran (THF) ($\log S_{\text{avg,RS}} = 15.30$) > quinoline (14.79) > DMSO (14.73) > diethylether (14.51) > 1,4-dioxane (14.42) and for ACNs: DMSO (17.53) > 1,4-dioxane (16.29) > tetrahydrofuran (15.93) > quinoline (15.50) > diethylether (13.52) (Fig. S7 and Tables S18-S19). These results can be described as a combination of the results obtained with HSP and the static calculations. This can be ascribed to the fact that a COSMO-RS calculations starts with the COSMO implicit solvation model, but combined with the post-processing method of breaking down the molecular surface into infinitesimal charge density areas, which leans more toward the HSP method. More remarkably is the absence of any alcohol solvents for both natural dye subclasses. The selected alcohols (Table S1) only showed an average $\log S_{RS}$ values of 9.98 and 11.22 for ACDs and ACNs, respectively. This indicates that the ACDs and ACNs would be about 5.32 and 6.32 times less soluble ($\log S_{RS}$ difference), respectively, compared to the best solvent from the screening (ACDs: THF and ACNs: DMSO). It can be noticed that these most optimal solvents are solely hydrogen bond acceptors and cannot act as hydrogen bond donors.

The aforementioned conclusion can be validated by superimposing σ -profiles of the solvents and ACDs or ACNs. Fig. 4A compares the σ -profiles of Cy and Cy3Glc based on the results obtained via the relative solubility screening ($\log S_{RS}$). The difference in σ -profiles between Cy and Cy3Glc is the higher intensity at both ends of the σ -profile. This can be ascribed to the presence of four additional hydroxy groups and ether functionality of the glucose moiety, which offers more hydrogen bonding sites. The profiles also showed the hydrogen acceptor ability ($\sigma > 0.0081 \text{ e}/\text{\AA}^2$) of the optimal solvents, i.e. lone electron pairs of oxygen or nitrogen that serve as electron donors, which improves the hydrogen bonding between solvent and dye. Furthermore, the hydrophobic part of the solvents' σ -profiles also showed good overlap with Cy's profile.

When the σ -profiles were evaluated by using the normalized "sigma match similarity" method [39], the highest similarity values with ACDs were found for m-cresol (0.104) > n-butylacetate (0.0874) > benzylalcohol (0.0835) > acetophenone (0.0819) > benzaldehyde (0.0775) and for ACNs: DMSO (0.0711) > 1,2-ethanediol (0.0672) > 2-methoxyethanol (0.0477) > dioxane (0.0350) > water (0.0331). Fig. 4B-C illustrate the σ -profiles of the five best solvents based on the degree of similarity with the Cy and Cy3Glc σ -profiles. It shows that the most optimal solvents for dissolving Cy are mainly based on hydrophobic interactions via electron rich aromatic systems; and hydrogen bonds. In the case of Cy3Glc, solvents with both electron donor ($\sigma > 0.0081 \text{ e}/\text{\AA}^2$) and electron acceptor ($\sigma < 0.0081 \text{ e}/\text{\AA}^2$) abilities are highly ranked such as 1,2-ethanediol, 2-methoxyethanol and water. Based on the "sigma match similarity" method, the results correlate closer to HSPs and follows the "like dissolves like" principle, but the highest solubility values are still obtained via the relative molar solubility method ($\log S_{RS}$).

3.4. Comparison of the different theoretical tools for ACDs and ACNs extraction

In Table 3, the most promising solvents for ACDs and ACNs as predicted by the different models are shown. After evaluating four predictive models (HSP, χ_{12} , DFT and COSMO-RS), it can be concluded that the different models predict different optimal solvents. Both group contribution methods (HSP and χ_{12}) displayed similar reoccurring solvents such as 1,2-ethanediol, ethanol and DMSO, but the χ_{12} -values also showed water as the best solvent for ACDs

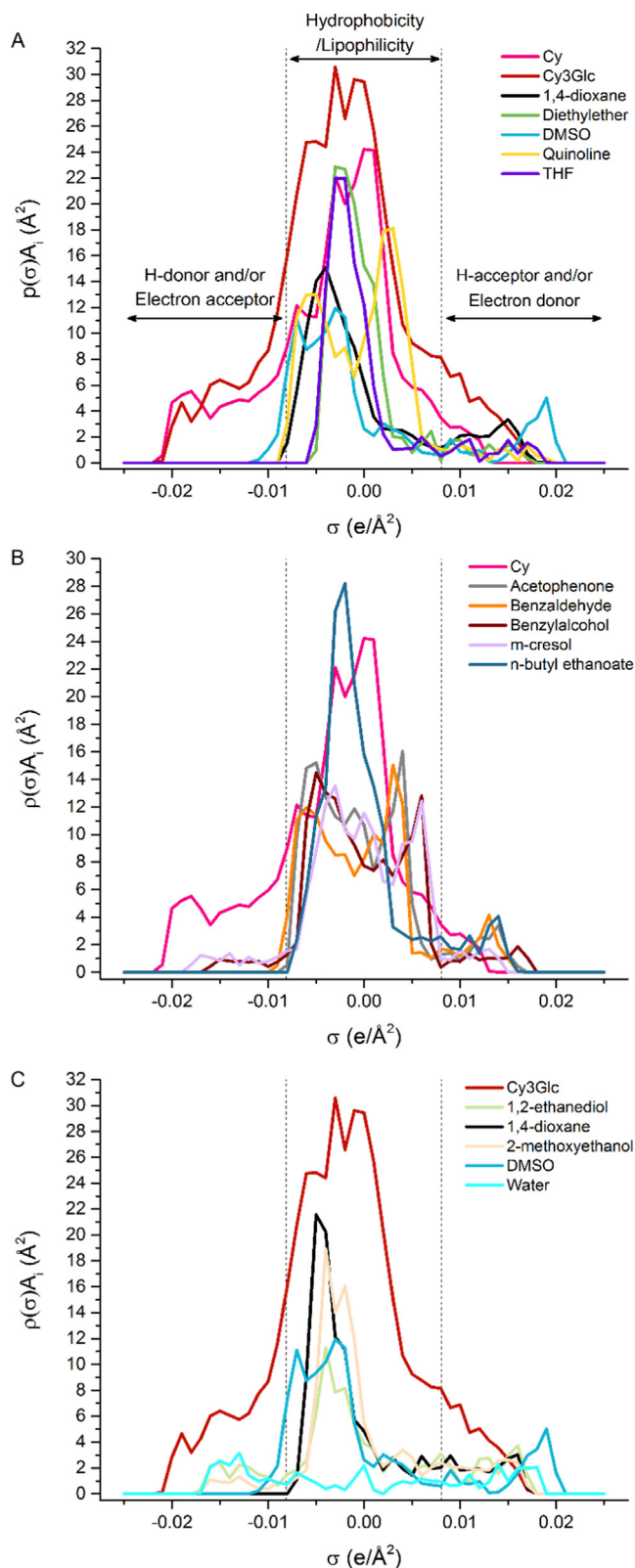


Fig. 4. Superimposed σ -profiles of Cy and Cy3Glc with the five most optimal solvents based on $\log S_{RS}$ (A) or σ -profile similarity (B, C). σ -values higher than 0.0081 $\text{e}/\text{\AA}^2$ show electron donor abilities, σ -values below 0.0081 $\text{e}/\text{\AA}^2$ show electron acceptor abilities and values in between indicate hydrophobic interactions.

and ACNs extraction. The latter contradicts the observed experimental trend that adding organic solvents improve the anthocyanin solubility. Hong et al. (2015) [42] have found a good

Table 3

The comparison of the five most interesting solvents for anthocyanidins and anthocyanins evaluated by the various predictive models (Figs. S3-S7).

Anthocyanidins (ACDs)				
HSP	χ_{12}	$\Delta G_{s,small}$	$\Delta G_{s,large}$	COSMO-RS
Ethylene glycol	Water	Methanol	Benzaldehyde	Tetrahydrofuran
m-Cresol	Glycol	Ethanol	Acetone	Quinoline
Benzylalcohol	Methanol	2-propanol	Acetonitrile	Dimethylsulfoxide
Dimethylsulfoxide	Ethanol	1-propanol	Quinoline	Diethylether
Ethanol	Dimethylsulfoxide	1-butanol	Acetophenone	1,4-dioxane
Anthocyanins (ACNs)				
HSP	χ_{12}	$G_{s,small}$	$G_{s,large}$	COSMO-RS
Ethylene glycol	Water	Methanol	Acetone	Dimethylsulfoxide
Dimethylsulfoxide	Glycol	Ethanol	2-propanol	1,4-dioxane
m-Cresol	Methanol	Water	Benzaldehyde	Tetrahydrofuran
Benzylalcohol	Ethanol	2-propanol	Ethanol	Quinoline
Ethanol	Dimethylsulfoxide	1-propanol	Acetonitrile	Diethylether

correlation between the chromaticity analyses of *Gardenia* extracts, which contain crocin, and the χ_{12} parameter. A higher color absorbance was observed for smaller χ_{12} -values. However, these χ_{12} -values ranged from 1.74 to 5.62 for the studied solvents, which technically indicates immiscibility. This questions the relevance of this method to non-polymer solutions. Solvation free energies based on DFT calculations favor alcohols and electron rich systems (e.g., aromatic rings and acetonitrile), while COSMO-RS recommends solvents with solely hydrogen bond acceptor abilities such as DMSO and ethers. COSMO-RS has shown a higher accuracy for solubility calculations on pure molecules compared to HSP and has been successfully applied for the solubility prediction of flavonoids in a wide variety of ionic liquids [43,44]. Therefore, further in-depth analyses of individual ACDs and ACNs solubilities obtained with COSMO-RS were carried out.

Fig. 5 focuses on the types of ACD and ACN extracted with water, the three traditional organic solvents and the most recommended solvents according to COSMO-RS. DMSO is predicted as ideal solvent for extracting Cy3Glc, but for Mv THF would be more recommended. From the traditional organic solvents, acetone is a better solvent in general to solubilize both ACDs ($\log S_{avg}$,

$R_S = 11.60$) and ACNs (12.51). The difference between ethanol and methanol lies in the fact that the former shows a 3-fold higher average solubility value (S_{RS}) for ACDs, while the latter is a better solvent for solubilizing ACNs with a 33% higher S_{RS} -value (Table 4). This confirms the results of Ju and Howard (2003) [18], who found that extraction of ACNs with methanol is 10% and 30% more effective than ethanol and water, respectively; and Metivier et al. (1980) [45] who obtained a 20% and 73% more effective ACNs extraction with methanol compared to ethanol and water, respectively. The solubility gap between the organic solvents acetone ($F(1,26) = 72.691$, $p < 0.001$), ethanol ($F(1,26) = 45.714$, $p < 0.001$) and methanol ($F(1,26) = 39.934$, $p < 0.001$) with water is already significant (Fig. 5). This extends even more for the most optimal solvents compared to the traditional organic solvents. However, from the five most optimal solvents, only DMSO would be viable in ACDs and ACNs extraction according to the GSK and CHEM21 solvent selection guides, which rank the solvent according to environmental, health and safety issues [46,47]. DMSO has a boiling point of 189 °C, which is not attractive in terms of solvent recovery. Within aqueous solutions, three-stage distillation technology has been applied for DMSO recovery, but it is very energy-intensive

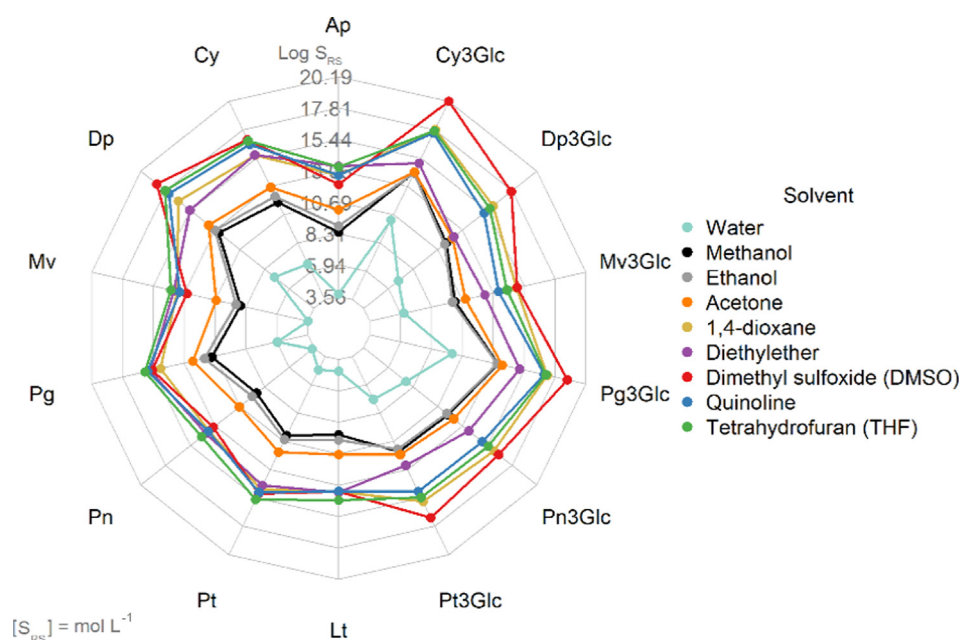


Fig. 5. The anthocyanin profiles, obtained via COSMO-RS, in terms of $\log S_{RS}$ between the five most optimal solvents and the traditional solvents (methanol, ethanol and acetone) used in anthocyanin extraction.

Table 4

The selectivity between the glycoside-aglycone pairs in terms of solubility ratios obtained with COSMO-RS. The figures represent the number of times a glycoside is more soluble compared to the aglycone in a selection of solvents, with Dp and Dp3Glc as exception.

Solubility ratio	DMSO	Ethanol	Methanol	Acetone	Water
$\log(S_{RS,Cy3Glc}/S_{RS,Cy})$	3.20	1.95	2.50	1.31	3.67
$\log(S_{RS,Dp}/S_{RS,Dp3Glc})$	0.91	1.73	1.21	1.57	0.47
$\log(S_{RS,Mv3Glc}/S_{RS,Mv})$	2.03	0.83	1.39	0.33	2.63
$\log(S_{RS,Pg3Glc}/S_{RS,Pg})$	3.22	1.89	2.49	1.34	4.01
$\log(S_{RS,Pn3Glc}/S_{RS,Pn})$	1.44	2.05	2.59	1.48	3.90
$\log(S_{RS,Pt3Glc}/S_{RS,Pt})$	2.38	0.81	1.36	0.23	2.47

as the majority of water needs to be evaporated. Selective adsorption to hydrophobic metal-organic frameworks is a potential alternative pathway [18]. Furthermore, the residue after extraction may not be suitable anymore for animal feed without intensive stripping. The CHEM21 solvent selection guide also allows the evaluation of less common solvents that are derived from lignocellulosic biomass (e.g., 2-methyl-tetrahydrofuran, cyrene, etc.) or natural sources (e.g., limonene from citrus waste) [47].

Table 4 illustrates the selectivity, displayed in Fig. 5, between the glycoside-aglycone pairs within these traditional solvents and DMSO. It shows that the highest selectivity can be obtained with pure water and DMSO. The glycosides of Cy, Mv, Pg, Pn, Pt are at least 2.47 times more soluble in water compared to the aglycones. These ratios are smaller for acetone, ethanol and methanol. Only the solubility ratio of Dp is smaller in water compared to ethanol. The claim in literature about higher solubilities for ACDs in alcohols than ACNs (glucosides) and the latter being highly soluble in water is valid for all ACDs and ACNs except for the pair Dp and Dp3Glc [20]. This underlines again the significant role of the glucose moiety in the solvation process via hydrogen bonds.

In literature, the polarity of ACDs and ACNs, based on retention order within reverse phase chromatography, show a decreasing trend in the order of Dp, Cy, Pt, Pg, Pn, and Mv [48]. In the case of ACDs, this correlates most closely with the solubility values predicted with COSMO-RS. The number of hydroxy groups on the B-ring has clearly got the highest impact on the solubility (Dp: 3 OH groups, Cy: 2 OH groups and Pg: 1 OH group). Pt, having 2 OH groups and 1 methoxy group showed higher water solubility than the 3-deoxyanthocyanidins (Ap and Lt). The increasing number of methoxy groups on the B-ring is unfavorable for water solubility. The polarity trend for ACNs can be more closely described by the solvation energies for large molecules ($\Delta G_{s,large}$) than the COSMO-RS model.

3.5. Binary mixtures

Mixed solvents play important roles in chemical syntheses and in extractions. Their change in polarity and Brønsted acidity and basicity can be decisive in the extraction outcome [40]. However, mixed solvents are difficult to describe as a homogenous medium in implicit solvation models. The preferential solvation behavior, which represents the complex ordering of co-solvents near the solute, is still challenging to include in implicit solvation model for polar or ionic compounds. Hybrid solvation models such as COSMO-RS are closest to describe mixed solvents without the need of an explicit solvent model which requires a higher degree of parametrization and are computationally more costly [40]. As previously mentioned, acetone, ethanol and methanol are the main organic solvents applied for ACDs and ACNs extraction in literature. Fig. S1 shows that pure organic solvents or aqueous mixtures containing 50, 70 and 80 vol% of organic solvent are mostly applied. However, higher fractions of organic solvent do not guarantee higher ACN content (Tables 1–2). Fig. 6A illustrates the relative solubility values of ACDs and ACNs for the aforementioned

ratios, determined with COSMO-RS, in acetone–water, ethanol–water and methanol–water mixtures. The solubility in binary mixtures follows the same trend compared to pure solvents: acetone > methanol > ethanol. A detailed look on the ACDs and ACNs profile for acetone–water mixtures shows that for Cy3Glc, Dp3Glc, Pg3Glc, Pn3Glc and Pt3Glc pure acetone performs more inefficient compared to an aqueous mixture of 90% v/v acetone (Fig. 6A and section S8 of Supporting Information). The anthocyanin profiles for the three solvents are relatively similar and show a linear increase in solubility with increasing volume fraction of organic solvent, which contradicts the trends observed within experiments (Tables 1 and 2). Catena et al. (2020) [49] also observed this linear correlation with COSMO-RS for the investigation of phenolic and anthocyanin compounds from *Oryza sativa* L. in ethanol–water mixtures.

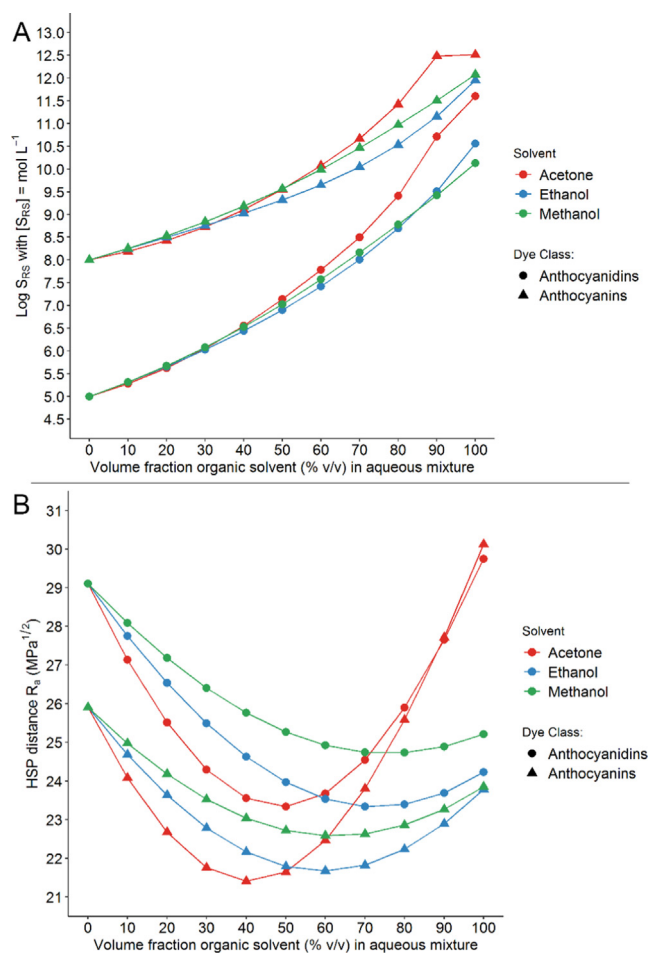


Fig. 6. Relative solubility values ($\log S_{RS}$) calculated with COSMO-RS (A) and solubility parameter distances R_0 (MPa^{1/2}) (B) of aqueous mixtures (acetone–water, ethanol–water and methanol–water) for ACDs and ACNs extraction.

Therefore, additional solubility parameter distances, based on HSPs, with increasing volume fraction of organic solvent, were calculated (section S9 of Supporting Information). Fig. 6B clearly illustrates the optimal ratio of binary aqueous mixtures for ACDs and ACNs. It was found that an aqueous mixture of acetone showed the shortest distance with ACDs at 50% v/v and ACNs at 40% v/v. For ethanol, a 70% v/v mixture is favored for ACDs and a 60% v/v for ACNs. The shortest distances between ACDs and methanol–water mixtures are found at 70–80% v/v and in the case of ACNs, 60%–70% v/v. Furthermore, statistical analyses also displayed that relative molar solubility ($\log S_{RS}$) of aqueous mixtures of acetone till 40% v/v are not significantly different compared to water (40% v/v acetone: $F(1,26) = 3.046$, $p = 0.093$; 50% v/v acetone: $F(1,26) = 5.940$, $p = 0.022$; 60% v/v acetone: $F(1,26) = 10.415$, $p = 0.003$) (Fig. S8). The same trend is observed for aqueous mixtures ethanol and methanol (40% v/v ethanol or methanol: $F(1,26) = 2.643$, $p = 0.116$; 50% v/v ethanol or methanol: $F(1,26) = 4.613$, $p = 0.041$; 60% v/v ethanol or methanol: $F(1,26) = 7.559$, $p = 0.011$; 70% v/v ethanol or methanol: $F(1,26) = 10.415$, $p = 0.002$). Whereas COSMO-RS is able to give quantitative information on the solubility behavior within various pure solvents, it is unable to accurately describe the solubility behavior within organic solvent–water mixtures. Therefore, HSPs are a more appropriate tool to find the most optimal mixture ratio.

3.6. Matrix compounds

During the extraction of ACDs and ACNs, various matrix compounds can be co-extracted. Therefore, the solubilities of glucose and pectin were calculated. These compounds are hydrophilic and thus, highly water soluble due to dipole interactions and hydrogen bonding. When analyzing the solubility values for both compounds in pure solvents with HSP, the R_s distances are generally smaller compared to ACDs and ACNs. The HSP method indicates that alcohols have the highest affinity for glucose and pectin (Table S6 and Fig. S3). This is in contrast to literature that indicates that both compounds would be more soluble in water. Alcohols such as ethanol or 2-propanol are frequently applied as precipitating agents for pectins. The presence of the alkyl group in alcohols lowers their polarity and hydrogen bonding ability with respect to water [50]. From the COSMO-RS screening, it can be observed that pectin has a higher solubility compared to glucose within the recommended solvents obtained from the COSMO-RS screening of ACDs and ACNs (Fig. 7 and Table S19). The sigma pro-

files show that aprotic polar solvents with electron-donor capability, such as 1,4-dioxane and dimethyl sulfoxide ($\log S_{RS} = 13.35$ and $\log S_{RS} = 9.79$) have higher capacity of dissolving pectin (Fig. S9). However, both hydrogen bond and acceptor capabilities of the solvent are required to sustain the hydrophilic interactions between pectin and solvent. Furthermore, the degree of methylation, molecular weight, pH, temperature and ionic strength also determine the pectin solubility [50]. Water is predicted to be the best solvent to extract glucose ($\log S_{RS} = 2.93$) while the slightly apolar character of alcohols compared to water results in a lower solubility ($\log S_{RS} \leq 0.69$). According to the model results, glucose is 175, 606 and up to 2000 times more soluble in water compared to methanol, ethanol and acetone, respectively (Fig. 7). This behaviour was also observed experimentally in binary aqueous mixtures for which the solubility of glucose decreases with increasing ethanol content [51]. This trend could not be reproduced with HSP where the solubility reaches a maximum at 70% v/v (Fig. S10A). Meanwhile, COSMO-RS gives a better representation on the solubility behaviour of glucose in higher organic solvent content (Fig. S10B).

4. Conclusions

In this work, the capabilities and limitations of several theoretical tools for the solubility determination of anthocyanidins and anthocyanins were evaluated. The Hansen solubility parameters appeared to be most appropriate to find the most optimal organic solvent–water mixture ratio for anthocyanidin and anthocyanin solubilities. This method showed that an aqueous mixture of 50% and 40% of acetone is optimal for anthocyanidins and anthocyanins, respectively. For ethanol, a 70% v/v aqueous mixture is favored for anthocyanidins and a 60% v/v for anthocyanins. The shortest Hansen solubility parameter distances between anthocyanidins and methanol–water mixtures are found at 70–80% v/v and in the case of anthocyanins, 60%–70% v/v. The Flory-Huggins parameter (χ_{12}) and solvation free energies showed moderate correlation with experimental literature values. The former overestimated the contribution of water, while the solvation energies give a general indication on the most interesting solvents. COSMO-RS is able to provide quantitative information on the solubility behavior within various pure solvents and describe the main intermolecular interactions between colorant and solvent. The relative molar solubility values showed that acetone is a better solvent to solubilize both anthocyanidins ($\log S_{avg,RS} = 11.60$) and anthocyanins ($\log S_{avg,RS} = 12.51$). The difference between ethanol

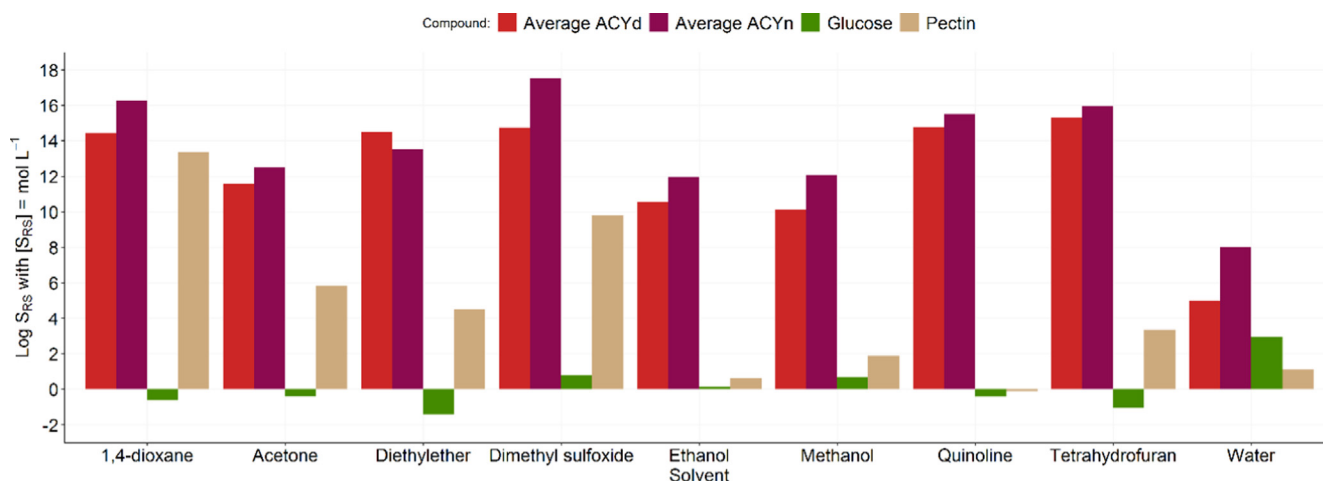


Fig. 7. Relative solubility values $\log S_{RS}$ (with $S_{RS} = \text{mol L}^{-1}$) for anthocyanidins, anthocyanins, glucose and pectin within the recommended solvents obtained from COSMO-RS solvent screening on anthocyanidins and anthocyanins (Fig. 4 and section S7).

and methanol lies in the fact that the former shows a 3-fold higher average solubility value (S_{RS}) for anthocyanidins, while the latter is a better solvent for solubilizing anthocyanins with a 33% higher S_{RS} -value. Furthermore, the solvent screening showed that electron rich aromatic compounds (i.e., π - π interactions) and compounds containing electron donors such as 1,4-dioxane, diethylether, DMSO, quinoline or tetrahydrofuran, solely acting as hydrogen bond acceptors, are favored from physicochemical perspective, but might not be chosen due to environmental considerations. Apart from the main dye components, these tools also allow to give an indication about co-extraction of components such as glucose and pectin. The results obtained from these various theoretical tools can be used as a benchmark for compound specific extractions or to find alternative 'green' solvents. It is thus of high significant added value in extractions from biomass or fermentation broths and can help steering experimental work to be more effective.

Declaration of Competing Interest

The authors declare that they have no known competing financial interests or personal relationships that could have appeared to influence the work reported in this paper.

Acknowledgments

The authors would like to thank the Research Board of Ghent University (BOF) for their financial support. The computational resources (Stevin Supercomputer Infrastructure) and services used in this work were provided by the VSC (Flemish Supercomputer Center), funded by Ghent University, FWO and the Flemish Government – department EWI.

Appendix A. Supplementary data

Supplementary data to this article can be found online at <https://doi.org/10.1016/j.molliq.2022.118606>.

References

- [1] I. Ignat, I. Volf, V.I. Popa, A critical review of methods for characterisation of polyphenolic compounds in fruits and vegetables, *Food Chem.* 126 (4) (2011) 1821–1835, <https://doi.org/10.1016/j.foodchem.2010.12.026>.
- [2] J.R. León-Carmona, A. Galano, J.R. Alvarez-Idaboy, Deprotonation routes of anthocyanidins in aqueous solution, pKa values, and speciation under physiological conditions, *RSC Adv.* 6 (58) (2016) 53421–53429, <https://doi.org/10.1039/C6RA10818K>.
- [3] O. Dangles, J.A. Fenger, The Chemical Reactivity of Anthocyanins and Its Consequences in Food Science and Nutrition. *Molecules* (Basel, Switzerland) 23 (8) (2018), <https://doi.org/10.3390/molecules23081970>.
- [4] Ø.M.M. Andersen, K.R. Markham, *Flavonoids: chemistry, biochemistry, and applications*: Taylor & Francis Group, LLC, 2006.
- [5] A. Castaneda-Ovando, M.D. Pacheco-Hernandez, M.E. Paez-Hernandez, J.A. Rodríguez, C.A. Galan-Vidal, Chemical studies of anthocyanins: A review, *Food Chem.* 113 (4) (2009) 859–871, <https://doi.org/10.1016/j.foodchem.2008.09.001>.
- [6] M. Shahid, Shahid-ul-Islam, F. Mohammad, *Recent advancements in natural dye applications: a review*, *J. Clean Prod.* 53 (2013) 310–331.
- [7] S. Zafra-Stone, T. Yasmin, M. Bagchi, A. Chatterjee, J.A. Vinson, D. Bagchi, Berry anthocyanins as novel antioxidants in human health and disease prevention, *Mol. Nutr. Food Res.* 51 (6) (2007) 675–683, <https://doi.org/10.1002/mnfr.200700002>.
- [8] S. Farrow, P.M. Rose, M. Benohoud, R.S. Blackburn, C.M. Rayner, Enhancing the Potential Exploitation of Food Waste: Extraction, Purification, and Characterization of Renewable Specialty Chemicals from Blackcurrants (*Ribes nigrum* L.), *J. Agric. Food Chem.* 66 (46) (2018) 12265–12273, <https://doi.org/10.1021/acs.jafc.8b04373>.
- [9] G.-I. Hidalgo, M. Almajano, *Red Fruits: Extraction of Antioxidants, Phenolic Content, and Radical Scavenging Determination: A Review*, *Antioxidants* 6 (1) (2017) 7.
- [10] P. Heffels, F. Weber, A. Schieber, Influence of Accelerated Solvent Extraction and Ultrasound-Assisted Extraction on the Anthocyanin Profile of Different Vaccinium Species in the Context of Statistical Models for Authentication, *J. Agric. Food Chem.* 63 (34) (2015) 7532–7538, <https://doi.org/10.1021/acs.jafc.5b02255>.
- [11] O. Onur Tolga, D. İlhan, Y. Nurettin, Ş.A.T. İhsan Güngör, Ö.Z. Mehmet, H.S. Gönül, Antioxidant Activity, Sugar Content and Phenolic Profiling of Blueberries Cultivars: A Comprehensive Comparison, *Not Bot Horti Agrobot Cluj-Napoca* 46 (2) (2018), <https://doi.org/10.15835/nbha46211120>.
- [12] L.R. Larsen, J. Buerschaper, A. Schieber, F. Weber, Interactions of Anthocyanins with Pectin and Pectin Fragments in Model Solutions, *J. Agric. Food Chem.* 67 (33) (2019) 9344–9353, <https://doi.org/10.1021/acs.jafc.9b03108>.
- [13] J. Chandrasekhar, M.C. Madhusudhan, K.S.M.S. Raghavarao, Extraction of anthocyanins from red cabbage and purification using adsorption, *Food Bioprod. Process.* 90 (4) (2012) 615–623.
- [14] P. Jing, M.M. Giusti, Effects of Extraction Conditions on Improving the Yield and Quality of an Anthocyanin-Rich Purple Corn (*Zea mays* L.) Color Extract, *J. Food Sci.* 72 (7) (2007) C363–C368, <https://doi.org/10.1111/j.1750-3841.2007.00441.x>.
- [15] J.E. Cacace, G. Mazza, Optimization of Extraction of Anthocyanins from Black Currants with Aqueous Ethanol, *J. Food Sci.* 68 (1) (2003) 240–248, <https://doi.org/10.1111/j.1365-2621.2003.tb14146.x>.
- [16] M.L. Blackhall, R. Berry, N.W. Davies, J.T. Walls, Optimized extraction of anthocyanins from Reid Fruits' Prunus avium 'Lapins' cherries, *Food Chem.* 256 (2018) 280–285, <https://doi.org/10.1016/j.foodchem.2018.02.137>.
- [17] R. Chirinos, H. Rogez, D. Campos, R. Pedreschi, Y. Larondelle, Optimization of extraction conditions of antioxidant phenolic compounds from mashua (*Tropaeolum tuberosum* Ruiz & Pavón) tubers, *Sep. Purif. Technol.* 55 (2) (2007) 217–225.
- [18] Z.Y. Ju, L.R. Howard, Effects of solvent and temperature on pressurized liquid extraction of anthocyanins and total phenolics from dried red grape skin, *J. Agric. Food Chem.* 51 (18) (2003) 5207–5213, <https://doi.org/10.1021/jf0302106>.
- [19] W. Wang, J. Jung, E. Tomasino, Y. Zhao, Optimization of solvent and ultrasound-assisted extraction for different anthocyanin rich fruit and their effects on anthocyanin compositions, *LWT-Food Sci. Technol.* 72 (2016) 229–238, <https://doi.org/10.1016/j.lwt.2016.04.041>.
- [20] H.E. Khoo, A. Azlan, S.T. Tang, S.M. Lim, Anthocyanidins and anthocyanins: colored pigments as food, pharmaceutical ingredients, and the potential health benefits, *Food Nutr. Res.* 61 (1) (2017) 1361779, <https://doi.org/10.1080/16546628.2017.1361779>.
- [21] W. Wiczowski, D. Szawara-Nowak, J. Topolska, Red cabbage anthocyanins: Profile, isolation, identification, and antioxidant activity, *Food Res. Int.* 51 (1) (2013) 303–309.
- [22] T. Das, C.H. Mehta, U.Y. Nayak, Multiple approaches for achieving drug solubility: an in silico perspective, *Drug Discov. Today* 25 (7) (2020) 1206–1212, <https://doi.org/10.1016/j.drudis.2020.04.016>.
- [23] D.W. Van Krevelen, K. Te Nijenhuis, *Properties of polymers: their correlation with chemical structure; their numerical estimation and prediction from additive group contributions*, Elsevier (2009).
- [24] H.C.M. Hansen, *Solubility parameters: a user's handbook*, CRC Press, 2007.
- [25] I.H. Bell, E. Mickoleit, C.-M. Hsieh, S.-T. Lin, J. Vrabec, C. Breitkopf, A. Jäger, A Benchmark Open-Source Implementation of COSMO-SAC, *J. Chem. Theory Comput.* 16 (4) (2020) 2635–2646, <https://doi.org/10.1021/acs.jctc.9b01016>.
- [26] R.E. Skyner, J.L. McDonagh, C.R. Groom, T. van Mourik, J.B.O. Mitchell, A review of methods for the calculation of solution free energies and the modelling of systems in solution, *Phys. Chem. Chem. Phys.* 17 (9) (2015) 6174–6191.
- [27] S.N. Steinmann, P. Sautet, C. Michel, Solvation free energies for periodic surfaces: comparison of implicit and explicit solvation models, *Phys. Chem. Chem. Phys.* 18 (46) (2016) 31850–31861, <https://doi.org/10.1039/C6CP04094B>.
- [28] C.M. Hansen, 50 Years with solubility parameters—past and future, *Prog. Org. Coat.* 51 (1) (2004) 77–84, <https://doi.org/10.1016/j.porgcoat.2004.05.004>.
- [29] M.J. Frisch, G.W. Trucks, H.B. Schlegel, G.E. Scuseria, M.A. Robb, J.R. Cheeseman, et al. *Gaussian 16 Rev. B.01*. Wallingford, CT2016.
- [30] K. Phan, S. De Meester, K. Raes, K. De Clerck, V. Van Speybroeck, Van Speybroeck V. A Comparative Study on the Photophysical Properties of Anthocyanins and Pyranoanthocyanins, *Chem. – A Eur. J.* 27 (19) (2021) 5956–5971, <https://doi.org/10.1002/chem.202004639>.
- [31] A.D. Becke, Density-functional thermochemistry. III. The role of exact exchange, *J. Chem. Phys.* 98 (7) (1993) 5648–5652.
- [32] C. Lee, W. Yang, R.G. Parr, Development of the Colle-Salvetti correlation-energy formula into a functional of the electron density, *Phys. Rev. B.* 37 (2) (1988) 785–789, <https://doi.org/10.1103/PhysRevB.37.785>.
- [33] J. Tirado-Rives, W.L. Jorgensen, Performance of B3LYP Density Functional Methods for a Large Set of Organic Molecules, *J. Chem. Theory Comput.* 4 (2) (2008) 297–306, <https://doi.org/10.1021/ct700248k>.
- [34] A.V. Marenich, C.J. Cramer, D.G. Truhlar, Universal Solvation Model Based on Solute Electron Density and on a Continuum Model of the Solvent Defined by the Bulk Dielectric Constant and Atomic Surface Tensions, *J. Phys. Chem. B.* 113 (18) (2009) 6378–6396, <https://doi.org/10.1021/jp810292n>.
- [35] J. Ho, A. Klamt, M.L. Coote, Comment on the Correct Use of Continuum Solvent Models, *J. Phys. Chem. A.* 114 (51) (2010) 13442–13444, <https://doi.org/10.1021/jp107136j>.
- [36] J. Ho, M.Z. Ertem, Calculating Free Energy Changes in Continuum Solvation Models, *J. Phys. Chem. B.* 120 (7) (2016) 1319–1329, <https://doi.org/10.1021/acs.jpcc.6b00164>.

- [37] M. Riquelme, A. Lara, D.L. Mobley, T. Verstraelen, A.R. Matamala, E. Vöhringer-Martinez, Hydration Free Energies in the FreeSolv Database Calculated with Polarized Iterative Hirshfeld Charges, *J. Chem. Inf. Model.* 58 (9) (2018) 1779–1797, <https://doi.org/10.1021/acs.jcim.8b00180>.
- [38] A. Klamt, Conductor-like Screening Model for Real Solvents: A New Approach to the Quantitative Calculation of Solvation Phenomena, *J. Phys. Chem.* 99 (7) (1995) 2224–2235, <https://doi.org/10.1021/j100007a062>.
- [39] A. Benazzouz, L. Moity, C. Pierlot, V. Molinier, J.-M. Aubry, Hansen approach versus COSMO-RS for predicting the solubility of an organic UV filter in cosmetic solvents, *Colloids Surf. Physicochem. Eng. Aspects* 458 (2014) 101–109, <https://doi.org/10.1016/j.colsurfa.2014.03.065>.
- [40] A.M. Maldonado, Y. Basdogan, J.T. Berryman, S.B. Rempe, J.A. Keith, First-principles modeling of chemistry in mixed solvents: Where to go from here?, *J. Chem. Phys.* 152 (13) (2020) 130902, <https://doi.org/10.1063/1.5143207>.
- [41] J. Gupta, C. Nunes, S. Vyas, S. Jonnalagadda, Prediction of Solubility Parameters and Miscibility of Pharmaceutical Compounds by Molecular Dynamics Simulations, *J. Phys. Chem. B.* 115 (9) (2011) 2014–2023, <https://doi.org/10.1021/jp108540n>.
- [42] I.K. Hong, H. Jeon, S.B. Lee, Extraction of natural dye from Gardenia and chromaticity analysis according to chi parameter, *J. Indus. Eng. Chem.* 24 (2015) 326–332, <https://doi.org/10.1016/j.jiec.2014.10.004>.
- [43] Z. Guo, B.-M. Lue, K. Thomasen, A.S. Meyer, X. Xu, Predictions of flavonoid solubility in ionic liquids by COSMO-RS: experimental verification, structural elucidation, and solvation characterization, *Green Chem.* 9 (12) (2007) 1362–1373, <https://doi.org/10.1039/B709786G>.
- [44] A.P. Sánchez-Camargo, M. Bueno, F. Parada-Alfonso, A. Cifuentes, E. Ibáñez, Hansen solubility parameters for selection of green extraction solvents. *TrAC, Trends, Anal. Chem.* 118 (2019) 227–237, <https://doi.org/10.1016/j.trac.2019.05.046>.
- [45] R.P. Metivier, F.J. Francis, F.M. Clydesdale, Solvent extraction of anthocyanins from wine pomace, *J. Food Sci.* 45 (4) (1980) 1099–1100.
- [46] R.K. Henderson, C. Jiménez-González, D.J.C. Constable, S.R. Alston, G.G.A. Inglis, G. Fisher, J. Sherwood, S.P. Binks, A.D. Curzons, Expanding GSK's solvent selection guide – embedding sustainability into solvent selection starting at medicinal chemistry, *Green Chem.* 13 (4) (2011) 854.
- [47] D. Prat, A. Wells, J. Hayler, H. Sneddon, C.R. McElroy, S. Abou-Shehadeh, P.J. Dunn, CHEM21 selection guide of classical- and less classical-solvents, *Green Chem.* 18 (1) (2016) 288–296, <https://doi.org/10.1039/C5GC01008J>.
- [48] J.S. Barnes, H.P. Nguyen, S. Shen, K.A. Schug, General method for extraction of blueberry anthocyanins and identification using high performance liquid chromatography–electrospray ionization-ion trap-time of flight-mass spectrometry, *J. Chromatogr. A.* 1216 (23) (2009) 4728–4735, <https://doi.org/10.1016/j.chroma.2009.04.032>.
- [49] S. Catena, N. Rakotomanomana, P. Zunin, R. Boggia, F. Turrini, F. Chemat, Solubility study and intensification of extraction of phenolic and anthocyanin compounds from *Oryza sativa* L. 'Violet Nori', *Ultrason. Sonochem.* 68 (2020) 105231, <https://doi.org/10.1016/j.ultsonch.2020.105231>.
- [50] W.-X. Jiang, J.-R. Qi, Y.-X. Huang, Y. Zhang, X.-Q. Yang, Yang X-Q, Emulsifying properties of high methoxyl pectins in binary systems of water-ethanol, *Carbohydr. Polym.* 229 (2020) 115420, <https://doi.org/10.1016/j.carbpol.2019.115420>.
- [51] L.A. Alves, J.B. Almeida e Silva, M. Giuliatti, Solubility of d-Glucose in Water and Ethanol/Water Mixtures, *J. Chem. Eng. Data.* 52 (6) (2007) 2166–2170. <http://doi.org/10.1021/je700177n>.